Biophysical Journal Volume 81 December 2001 3204–3215

How the Loop and Middle Regions Influence the Properties of *Helicobacter pylori* VacA Channels

Francesco Tombola,* Cristina Pagliaccia,† Silvia Campello,* John L. Telford,† Cesare Montecucco,* Emanuele Papini,‡ and Mario Zoratti*

*Centro Biomembrane del Consiglia Nazionale delle Ricerche and Dipartimento di Scienze Biomediche, Università di Padova, Italy; †Istituto Ricerche Immunologicae Siena, CHIRON S.p.A., Siena, Italy; ‡Dipartimento di Scienze Biomediche e Oncologia Umana, Sezione di Patologia Generale, Università di Bari, Italy

ABSTRACT VacA is a pore-forming cytotoxin produced by *Helicobacter pylori* in several strain-specific isoforms, which have been classified in two main families, m1 and m2, according to the sequence of a variable "midregion." Both forms are associated with gastric pathologies and can induce vacuolation of cultured cells. The comparison of two representative toxins, m1 17874 and m2 9554, has indicated that the m2 form is less powerful in vacuolation assays and that its effects are more strongly cell type dependent. To rationalize these differences and to investigate structure-function relationships in this toxin, we have compared the properties of the channels formed by these two variants and by a construct derived from 17874 by deleting a loop that connects the two toxin domains, which is shorter in 9554 than in 17874. Although the channels formed by all three proteins are similar, m2 9554 channels have, on average, a lower conductance and are less anion-selective and more voltage-dependent than the m1 pores. Furthermore, the rate of incorporation of 9554 VacA into planar bilayers depends on lipid composition much more strongly than that of 17874. The comparison with the behavior of the loop deletion mutant indicates that this latter property, as well as a portion of the conductance decrease, may be attributed to the reduction in loop length. The differences in pore properties are proposed to account in part for the different cytotoxicity exhibited by the two toxin isoforms. We furthermore present evidence suggesting that the conformation of the membrane-embedded toxin may be influenced by the lipid composition of the membrane itself.

INTRODUCTION

Helicobacter pylori is believed to be a major causative agent of human peptic disorders including chronic gastritis and ulcers (Warren and Marshall, 1983; Marshall et al., 1985; Morris and Nicholson, 1987; Cover and Blaser, 1996; Parsonnet, 1998; Montecucco and Rappuoli, 2001). VacA, a secreted toxin, can induce the formation of large vacuoles in cultured cells (Leunk et al., 1988; Cover and Blaser, 1992; Montecucco et al., 1999a,b), and is believed to play an important role in the generation of epithelial damage. The mature form consists of an N-terminal (p37) and a C-terminal (p58) domain, linked by a protease-sensitive loop. In solution it forms hexa- or heptameric oligomers, as well as the corresponding dodecamers and tetradecamers (Lupetti et al., 1996; Cover et al., 1997; Lanzavecchia et al., 1998; Burroni et al., 1998), which dissociate at low (de Bernard et al., 1995; Cover et al., 1997) or high (Yahiro et al., 1999) pH values. This activating treatment enables the toxin to insert into phospholipid bilayers, where it is also present as oligomers (Molinari et al., 1998; Czajkowsky et al., 1999; Vinion-Dubiel et al., 1999; Pagliaccia et al., 2000), forming low-conductance, anion-selective, voltage-dependent channels (Tombola et al., 1999a; Iwamoto et al., 1999; Szabò et al., 1999). Vacuolation, as well as VacA-induced permeabilization of polarized epithelia, is linked to the activity of these channels (Tombola et al., 1999a,b; Szabò et al., 1999).

Our current mechanistic model for cell vacuolation envisions VacA binding, channel formation and internalization via the endocytic pathway. The presence of anion-selective channels in late endosomes stimulates the electrogenic V-ATPase with consequent accumulation of HCl, and, in the presence of permeable amines, of osmotically active ammonium salts. The ensuing swelling presumably primes the endosomes for Rab7 (Papini et al., 1997) and Rac1 (Hotchin et al., 2000) -dependent fusion and vacuole formation.

The *vacA* gene is polymorphic (Atherton et al., 1995, 1999; Cover, 1996). The most variable region corresponds to an ~300-amino acids midregion in the p58 domain ("m region"). The various m sequences have been grouped into two families of alleles, m1 and m2. Both types are pathogenic, but m2 toxins have a limited vacuolating activity on HeLa and on nonpolarized MDCK cells (Reyrat et al., 1999; Pelicic et al., 1999). On other cell lines, such as RK13 and primary human cells from gastric biopsies, both m1 and m2 forms are effective, but the latter is approximately four times less powerful on a molar basis (Pagliaccia et al., 1998). This different sensitivity has been rationalized in terms of differences in cell-toxin interaction. The two types of toxin are proposed to have distinct receptors, both of which would be present, e.g., on RK13 cells, whereas HeLa cells would expose only the m1-specific receptor.

Structural studies on the two toxin types, performed with the m1 forms 17874 and 60190 and with m2 9554, indicated

Received for publication 23 October 2000 and in final form 28 August 2001.

Address reprint requests to Mario Zoratti, CNR C.S. Biomembrane, Dipartimento Scienze Biomediche, Viale Giuseppe Colombo, 3, 35121 Padova, Italy. Tel: 39-049-8276054; Fax: 39-049-8276049; E-mail: zoratti@civ.bio.unipd.it.

0006-3495/01/12/3204/12 $2.00

that both types exist as oligomeric "rosettes" in solution. 17874 and 60190 can form both heptamers (~70 and 20%, respectively) and hexamers (Lupetti et al., 1996; Lanzavecchia et al., 1998; Czajkowsky et al., 1999). Only hexamers have been reported for mica-adsorbed 9554 (Cover et al., 1997). VacA 60190 seems to form only hexamers after dissociation and insertion into a supported lipid bilayer (Czajkowsky et al., 1999). The proportion of heptamers and hexamers appears to be related to the length of the loop connecting the p37 and p58 domains: the loops of 60190 and 9554 are shorter than that of 17874 by eight and five amino acids, respectively. When 16 amino acids are deleted from the loop of 17874 the percentage of heptamers drops from 70 to 20%, whereas a complete (46 residues) loop deletion leads to the exclusive formation of hexamers by the resulting m1del46 protein (Burroni et al., 1998).

Prompted by the finding that the cytotoxic properties of VacA are due to pore formation, we have extended the comparison between m1 and m2 forms to their electrophysiological properties to verify whether any correlation exists between possible differences in ion conduction and the different vacuolating power of the toxins and to obtain data for a structure-function correlation for the channel. To test the possibility that the length of the interdomain loop may influence channel properties, we have investigated also the properties of m1del46. Because all three toxin forms cause vacuolation, we expected them to produce channels with qualitatively similar properties.

MATERIALS AND METHODS

VacA forms m1 17874, m2 9554 (Pagliaccia et al., 1998), and m1del46 (Burroni et al., 1998) were purified as previously reported (Manetti et al., 1995) and stored at 0 to 4°C in phosphate-buffered saline (PBS) or 150 mM NaCl, 20 mM Hepes/Na, pH 7.0. Purified rabbit anti-VacA m1 17874 polyclonal immunoglobulin G (IgG) was from Chiron (Siena). Its affinities for m1 17874 and m1del46 (see Fig. 3 *A*) were compared by a modified enzyme-linked immunosorbent assay conducted in parallel. Briefly, a fixed amount (0.35 μg in 40 μl of PBS) of the toxins was seeded on 96-well plates and allowed to become absorbed overnight. After saturation with bovine serum albumin, fixed volumes of IgG solutions of variable concentrations were added and allowed to stand for 4 h at 37°C. The toxin-antibody complexes were exposed to secondary peroxidase-conjugated goat anti-rabbit antibodies (Calbiochem, San Diego, CA) for 1 h at 37°C. Reaction with *o*-dianisidine/H_2O_2 (Sigma, Milan, Italy) reagent was started, and the absorbance (405–540 nm) was measured after 5 min using a Packard SpectraCount and corrected for the corresponding blank (same procedure, no VacA) value. To measure binding of the toxins to HeLa cells by cytofluorimetry (see Fig. 3 *B*), the cells were detached when at 80% confluence by EDTA treatment. Aliquots (5×10^5 cells) were suspended in 100 μl of PBS and exposed to preactivated toxin (1 μg/ml) for 1 h at 4°C. The procedure of Massari et al. (1998) was then followed, using a saturating concentration of anti-VacA antibodies (20 μg/ml). Secondary fluorescein isothiocyanate-labeled goat antibodies were from DAKO (Glastrup, Denmark). A total of 1×10^4 gated events per sample were collected using a Coulter flow cytofluorimeter.

Planar bilayer experiments were conducted as previously reported (Tombola et al., 1999a,b, 2000). In all experiments the toxin was preactivated by incubation in PBS/HCl, pH $\approx$ 2, 37°C for 8 min immediately before being added to the bilayer apparatus chamber. Toxin was added into the compartment (*cis*) containing the active electrode, whose voltage relative to ground is reported. Currents (cations) flowing from the active to the ground electrode are defined as positive and plotted upwards. Diphytanoyl-phosphatidylcholine (DPhPC), phosphatidylcholine (PC), and phosphatidylethanolamine (PE) were from Avanti Polar Lipids (Alabaster, AL). Phosphatidylinositol (PI), phosphatidylserine (PS), phosphatidic acid (PA), and poly-L-lysin hydrobromide (molecular mass, 70–150 kDa) were from SIGMA (Milan, Italy). Soybean asolectin was either from SIGMA, type IIS, or from Avanti. Sources and stock solutions of inhibitors were as reported by Tombola et al. (1999b). The standard experimental medium was 500 mM KCl (2 M KCl for single-channel recordings), 0.5 mM $CaCl_2$, 0.5 mM $MgCl_2$, 10 mM Hepes/K, pH 7.2 (referred to below as "500 mM KCl" or "2 M KCl"). For reversal potential determinations the [KCl] gradient was 390 (*cis*): 100 (*trans*) mM. Rates of transmembrane current development were measured as previously (Tombola et al., 1999a). "Instantaneous" rectification ratios ($|I^+/I^-|$ or $|I^-/I^+|$) are defined as the absolute value of the ratio of the transmembrane current amplitude measured at a given potential over that measured at the opposite (same magnitude, opposite polarity) voltage. They were determined by applying trains of brief (seconds) square pulses of voltage of alternating polarity and increasing magnitude, separated by comparable periods at zero potential. When appropriate, current amplitudes measured in multichannel experiments were corrected for ongoing toxin incorporation as described (Tombola et al., 1999a).

K_D values for the inhibitors used were calculated from the best fit of titration data according to the equation $\%_{rc} = 100 - P_1/(1 + K_D/[L])$, in which $\%_{rc}$ stands for the percent residual current, $[L]$ is the concentration of inhibitor, and P_1 is a fitting parameter, whose physical meaning is the maximal percentage of inhibition theoretically observable at an infinite concentration of inhibitor (Tombola et al., 1999b). Each titration curve comprised at least five experimental points, each representing the average of at least three independent determinations. The approach of Tombola et al. (2000) was used to estimate the depth in the transmembrane electrical field (δ) of the binding site for 4,4′-diisothiocianato stilbene-2,2′-disulfonic acid in the m2 VacA channel. Briefly, estimates of the dissociation constant, K_D, at various voltages can be obtained from the fit of plots of the parameter $\Phi(|V|)$ versus $[DIDS]_{cis}$ (see Fig. 6 *C* in Results) according to the equation:

$$\Phi(|V|) \equiv |I^+/I^-|/|I^+/I^-|_0 = \{([DIDS]/K_D^- + 1)/([DIDS]/K_D^+ + 1)\} \quad (1)$$

in which $|I^+/I^-|$ is the rectification ratio measured at the given concentration of DIDS and absolute value of the potential, $|I^+/I^-|_0$ is the corresponding ratio in the absence of inhibitor, K_D^- and K_D^+ are the values of the dissociation constant at negative and positive potentials of absolute value $|V|$, respectively. An estimate of δ was then obtained, adopting Woodhull's two symmetrical barriers model (Woodhull, 1973; Hille, 1992), by fitting plots of K_D versus V according to the equation:

$$K_D = (k_{off}^{cis} + k_{off}^{trans})/k_{on}^{cis} = [b_{off}^{cis} \times \exp(-\delta zFV/2RT) + b_{off}^{trans} \times \exp((1 - \delta)zFV/2RT)]/b_{on}^{cis} \times \exp(\delta zFV/2RT) \quad (2)$$

In this equation the various b constants represent the rates of channel blocking ("on") or unblocking ("off") at zero voltage. For the "unblocking" reaction, different b constants characterize exit toward the *cis* compartment or in the opposite direction. b_{off}^{cis} and b_{off}^{trans} reflect both the intrinsic affinity of the binding site(s) for the ligand within the channel, and the kinetic parameters that characterize movement in one or the other direction, which are not equivalent because the channel is asymmetric (Tombola et

FIGURE 1 Comparison of the sequences of the loop and m regions of VacA m1, m2, and m1del46. (*A*) Scheme illustrating the toxin structure. (*B*) Sequences of the loop region (missing in m1del46). (*C*) Sequences of the m region (identical in m1 and m1del46). Black boxes comprise the conserved residues. Residues bordering the regions of interest are shown against a gray background. The numbers on the left identify the first residue shown on the same line, according to the sequence of the mature proteins.

al., 2000). Because DIDS was present only in the *cis* compartment in the relevant experiments, no "on" reaction from the *trans* side was considered.

RESULTS

We have analyzed the electrophysiological properties of three VacA forms: the relatively well-characterized m1 17874, the representative m2 9554 form, and the construct obtained from the former by deletion of the loop linking the p37 and p58 domains (m1del46; Burroni et al., 1998). Fig. 1 compares the sequences of the three proteins in the loop (1B) and m (1C) regions. These two regions together account for 74 to 83% of the total mutations and for 83 to 92% of the nonconservative mutations between m1 17874 and m2 9554 (ranges are given, rather than exact values, because the calculated percentages depend on the location of the C terminus of the isolated protein, which may vary because fragments of up to 15 KDa can be cleaved off the C-terminal domain (Nguyen et al., 2001)). Thus, any functional differences between the isoforms are likely to be determined by the changes in the sequences in one or both of these regions.

As previously reported (Tombola et al., 1999a), the formation of VacA 17874 channels in planar lipid bilayers is only slightly dependent on the composition of the membrane (Fig. 2 *C*). Fig. 2, *A* and *B*, shows that m2 9554 and m1del46 exhibited a strong preference for asolectin over DPhPC. The behavior was the same if a 1:1 PC:PE mixture was used instead of DPhPC, and it did not change if 10% (w/w) PA, PI, or PS were mixed with DPhPC or PC:PE (data not shown). Thus, the observed behavior cannot be ascribed to the presence of negatively charged phospholipids in asolectin. Due to these properties, the multichannel experiments reported below were all conducted with asolectin membranes, whereas single-channel experiments were performed in DPhPC, to maximize the time available for the observation of a single channel before the appearence of a second one. Quantitative comparisons of rates of incorporation by different toxin forms are difficult, because these rates vary considerably from preparation to preparation and depend on the time elapsed from purification for unknown reasons.

A factor influencing the rate of m1 channel formation (transmembrane current development) is voltage: the rate of transmembrane conductance increase is higher at voltages negative on the side of toxin addition (*cis*) (Tombola et al., 1999a). This was found to be the case also with m2 and m1del46 (Fig. 2 *D*). As indicated by the comparison with the instantaneous rectification ratios, the effect of voltage does not reflect only the intrinsic voltage dependence of the pores but indicates instead a specific effect of the electrical field on the incorporation of the toxin.

Pagliaccia et al. (1998) investigated m2 9554 binding to HeLa cells and found it to be weak. A direct comparison with m1 17874 was made difficult by the fact that the available polyclonal antibodies versus the two forms cross-react poorly (Pagliaccia et al., 1998). The affinities for VacA 17874 and m1del46, instead, turned out to be nearly the same (Fig. 3 *A*), thus allowing the comparative evaluation of toxin binding by flow cytofluorimetry (Fig. 3 *B*). Binding of VacA del46 turned out to be ~40% of that of its parent toxin (Fig. 3 *B*, *insert*). Vacuolation assays on the other hand revealed no statistically significant difference between the two toxins, confirming the previous report by Burroni et al. (1998) (data not shown).

As expected, the properties of the channels of the three types, as deduced from multichannel experiments, turned out to be similar, although not identical. Fig. 4 illustrates this for voltage dependence (*A* and *B*) and selectivity between K^+ and Cl^- (*C* and *D*). The voltage-dependence of VacA 9554 is somewhat steeper than that of 17874, whereas that of m1del46 is practically identical to that of its parent protein. The m2 form also appears to be less selective than

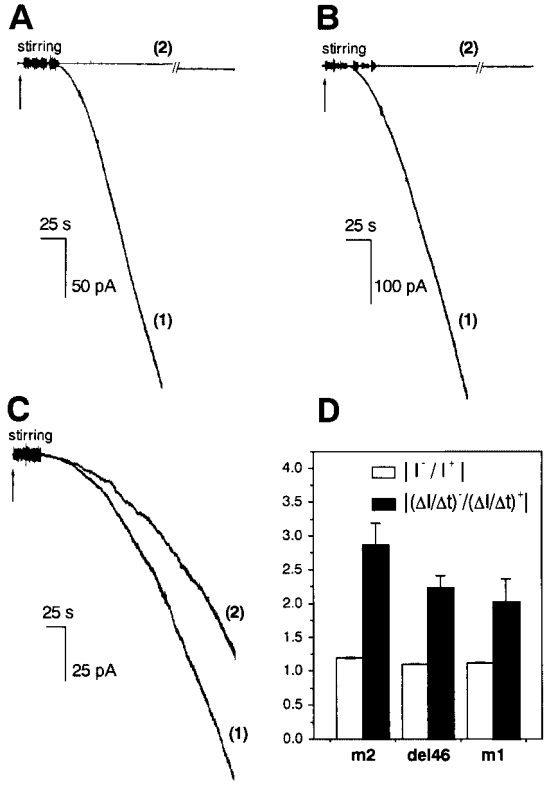

FIGURE 2 Effect of membrane composition and voltage on the rate of channel formation by different VacA forms. (*A–C*) Current records from planar bilayer experiments conducted with symmetrical 500 mM KCl at −40 mV. Toxin addition is indicated by arrows. The traces shown in each panel were recorded on the same day, using the same toxin preparation, and under identical conditions except for membrane composition. The curves labeled (*1*) were recorded with membranes made of asolectin; those labeled (*2*) were recorded with membranes made of DPhPC. (*A*) m2 VacA 9554, 20 nM. The break in trace 2 corresponds to 15 min. (*B*) m1del46, 20 nM. The break in trace 2 corresponds to 20.5 min. (*C*) m1 VacA 17478, 10 nM. (*D*) Voltage-dependence of the rate of current development in asolectin. Pore formation is favored by negative voltages. The black histograms compare the ratios $(\Delta I/\Delta t)^-/(\Delta I/\Delta t)^+$ ((rate of current increase at −40 mV)/(rate of current increase at +40 mV)) for the three toxin forms. The rates were measured as the slope of recordings similar to those in Fig. 1, *A* through *C* in the semilinear portion of sigmoidal traces. The voltage was repeatedly switched between positive and negative values within each experiment. The values plotted are the mean ± SE of five (m1), nine (m2), and eight (m1del46) determinations. The white histograms report the instantaneous current rectification ratios ($|I^-/I^+|$) at $|V| = 40$ mV. In this case the means of 16 (m1 17874), 25 (m2 9554), and 10 (m1del46) determinations are reported. Membrane, asolectin; medium, symmetrical 500 mM KCl.

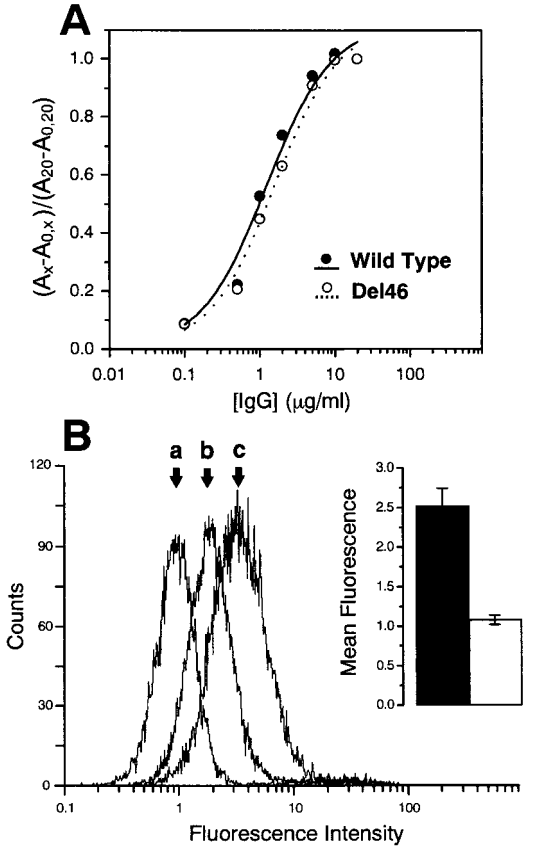

FIGURE 3 Comparison of m1 17874 and del46 VacA binding to HeLa cells. See Materials and Methods for details. (*A*) The primary antibody has similar affinities for both toxin forms. The ordinate values are the ratio of the absorbance measured with *X* μg/mL IgG, corrected for the corresponding VacA-less blank, over that measured with 20 μg/mL, also corrected. (*B*) Representative flow cytometric fluorescence histograms showing the distribution of VacA on HeLa cells. (*a*) Control (cells treated with antibodies only); (*b*) del46-treated cells; (*c*) 17874-treated cells. (*Inset*) Mean fluorescence values, calculated from curves such as those shown and corrected by subtracting the control value, were averaged and are plotted with mean ± SE ($n = 4$). Black column, 17874-exposed cells; white column, del46-exposed cells.

17874 with an average E_{rev} of 27 ± 2 mV and a calculated P_{Cl}/P_K ratio of 10 ± 2 (the ratios reported are averages of the values calculated from the E_{rev} of each of seven individual experiments) to be compared with an average E_{rev} of 30.9 ± 1.4 mV and an average P_{Cl}/P_K of 24 ± 11 obtained for 17874 ($n = 18$; Tombola et al., 1999a). The difference is statistically significative ($p < 0.01$). On the contrary, the selectivity between Cl^- and K^+ displayed by m1del46 is not significantly different from that of 17874.

We compared the effectiveness of four VacA inhibitors, two "classical" blockers believed to follow an aqueous pathway into the channel (DIDS and 4-acetamido-4′-isothiocianato stilbene-2,2′-disulfonic acid (SITS)) and two amphiphilic compounds (5-nitro-2-(3-phenylpropylamino) benzoic acid (NPPB) and IAA-94). The results are reported in Table 1. The constants characterizing the inhibition of the m1 form from the *cis* side, which had been previously determined using DPhPC as the membrane lipid (Tombola et al., 1999b), were redetermined using asolectin to ensure homogeneity with the data pertaining to the other two toxin forms. The K_D for NPPB changed only slightly, whereas those for the other three compounds increased somewhat upon switching to asolectin (e.g., $K_D^{DIDS,\ cis}$ from 36 ± 2 to 65 ± 2 μM). The effect of NPPB, DIDS, or SITS added on

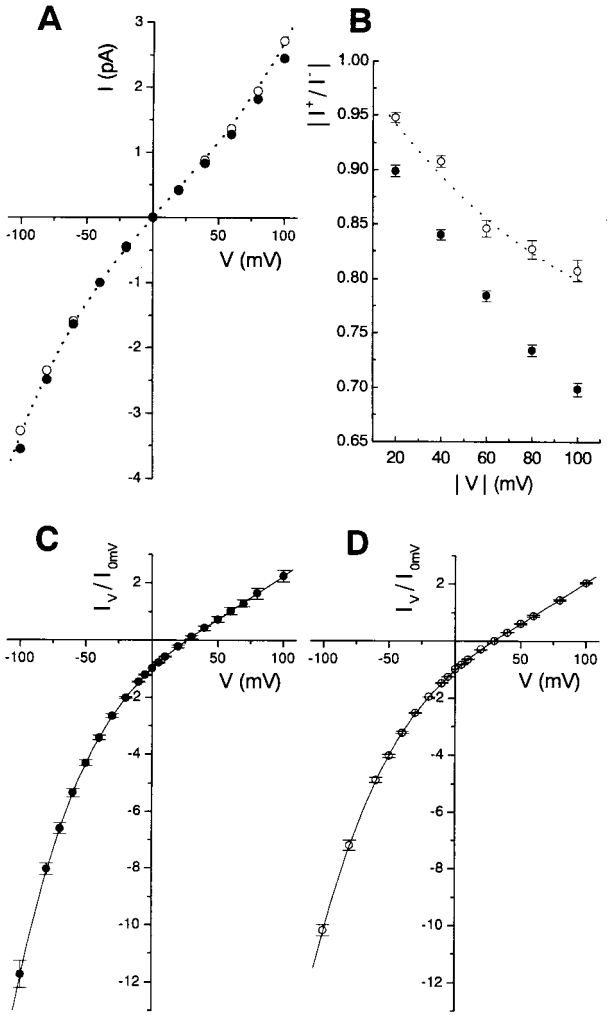

FIGURE 4 Voltage-dependence and selectivity of m1, m2, and m1del46 VacA are similar. (*A*) Representative I/V curves in symmetrical 500 mM KCl for m2 VacA 9554 (●) and m1del46 (○). The current values have been normalized for presentation purposes dividing them by the absolute value of the current flowing at −40 mV. The dotted line is the best polynomial fit of the data obtained for m1 VacA 17874 (Tombola et al., 1999a. (*B*) Plot of the rectification ratio, $|I^+/I^-|$, versus $|V|$. The mean ± SE of 25 (m2; ●) and 10 (m1del46; ○) experiments is shown. (*C*) Average ($n = 7$) I/V curve under asymmetrical salt conditions (390:100 mM KCl, *cis*:*trans*) for m2 VacA 9554. The data have been normalized by division by the absolute value of the current measured at 0 mV. The polynomial fit yields a reversal potential of 26.8 ± 1.2 mV. (*D*) As *C*, for m1del46 ($n = 3$); E_{rev}, 30.1 ± 1.0 mV.

the *trans* side was also investigated. As expected (Tombola et al. 2000), NPPB inhibited all three toxin forms to the same extent, irrespective of the side of addition. Two-hundred micromolars SITS in *trans* did not inhibit current conduction by any of the three toxin forms. In the case of m1 VacA, the only one for which the comparison could be carried out, this was true when using either asolectin or DPhPC. However, DIDS behaved differently. As shown in Fig. 5 *A*, the inhibition of m1 VacA produced by 200 μM

TABLE 1 Comparison of inhibition parameters

	m1 VacA 17874		m1de146 VacA		m2 VacA 9554	
Inhibitor	K_D (μM)	P_1	K_D (μM)	P_1	K_D (μM)	P_1
NPPB	21 ± 1	90 ± 1	58 ± 5	103 ± 3	50 ± 1	95 ± 2
DIDS	65 ± 2	99 ± 1	69 ± 5	97 ± 2	109 ± 6	103 ± 3
SITS	307 ± 10	98 ± 2	254 ± 29	96 ± 5	244 ± 16	97 ± 3
IAA-94	346 ± 31	80 ± 4	n.d.	n.d.	436 ± 47	89 ± 6

K_D and P_1 values (see Materials and Methods) for the inhibitors and VacA forms are indicated. Inhibitors were added on the *cis* side only. Membrane, asolectin; Medium, 500 mM KCl; Voltage, −40 mV. n.d. = not determined.

DIDS decreased from 79% (*cis*) to 31% (*trans*) when the membrane was made of DPhPC, but from 73% to 4.5% if the membrane was formed by asolectin. m2 and m1del46 VacA, in asolectin, were inhibited by *trans*-side DIDS even less efficiently ($\%_{inhib} < 2\%$) than m1 VacA.

According to the manufacturers, the major components of soybean asolectin are PC (~24%) and PE (18%). PI (12%) and PA (4%) are the major acidic phospholipids with other negatively charged lipids present in undetermined lower amounts. To verify whether the low extent of inhibition by *trans*-side DIDS could be attributed to the presence of negatively charged lipids in asolectin, we performed experiments in which 200 μM DIDS was added (*trans* side) to 500 mM KCl medium bathing m1 VacA-doped membranes made of PC:PE 1:1 or PC:PE 1:1 plus 20% (w/w) PI (Fig. 5 *B*). DIDS inhibited current conduction by 25% (PC+PE) and 16% (PC+PE+PI), respectively. We obtained a similar result using PS instead of PI (data not shown). Coherently, using asolectin, if 5 μg/ml poly-lysine was added to the *trans* chamber to mask negative charges, inhibition by *trans*-side DIDS was approximately twice as high as that of the control experiments (no poly-lysine added). We also studied the influence of ionic strength by determining the K_D for *cis*-side DIDS and m1 VacA in asolectin or DPhPC in symmetrical 0.1, 0.5, and 2 M KCl (Fig. 5 *C*). In asolectin, the parameter dropped going from the least to the most concentrated solution. The values determined using DPhPC were in all cases lower than those obtained with asolectin. Interestingly, K_D^{DPhPC} remained approximately constant going from 0.1 to 0.5 M KCl but then decreased, much like $K_D^{asolectin}$, going from 0.5 to 2 M salt. Possible interpretations of these observations are presented in the discussion section.

NPPB produced a voltage-dependent, but side-of-addition independent block, which has been proposed to arise from partitioning of the amphiphilic compound into the lipid bilayer, voltage-independent diffusion from the lipid phase to the blocking site inside the channel, and voltage-dependent efflux along the channel lumen (Tombola et al., 2000). In the case of m1 VacA 17874, the analysis of the voltage dependence of the rectification ratio led to an estimate of δ, the depth at which the binding site for NPPB is located in the transmembrane electrical field (Tombola et al., 2000). We attempted a similar analysis on m2 VacA

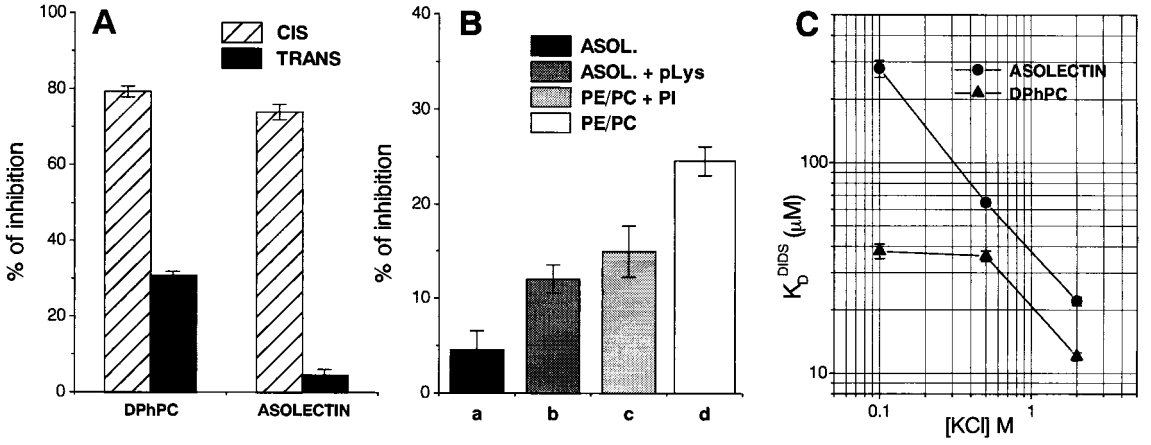

FIGURE 5 Effect of lipid composition and salt concentration on the inhibition of m1 VacA 17874 by DIDS. (*A*) Percentage of inhibition of current conduction caused by: 200 μM DIDS on the *cis* (*hatched columns*) or *trans* (*black*) side of an m1 VacA-containing membrane made of DPhPC (*left*) or asolectin (*right*). The averages of three to five experiments with associated mean ± SE are shown. Medium, symmetrical 500 mM KCl; *V*, −40 mV. (*B*) Inhibition by 200 μM DIDS (in *trans*) of the current conducted by VacA inserted in membranes of different lipid composition. The lipid used were (as indicated): asolectin, with or without 5 μg/ml poly-lysin added in *trans*, and PC:PE 1:1, with or without 20% (w/w) PI. Medium and voltage are as in *A*. Each value is the mean of at least three experiments mean ± SE. (*C*) Log-log plot of the K_D values for inhibition of m1 VacA 17874 by *cis*-side DIDS as a function of salt concentration and of membrane composition (●, asolectin; ▲, DPhPC). The data are averages of three experiments mean ± SE. Medium, 0.1, 0.5, or 2 M KCl; *V*, −40 mV.

9554 with the purpose of comparing the positions of the sites in m1 and m2 channels. As illustrated in Fig. 6 *A*, however, the slope of the curves relating the rectification ratio to $|V|$ was less affected by NPPB in the cases of m2 VacA 9554 (curves 1, 1′) and of m1del46 (curves 2, 2′) than in that of m1 (curves 3, 3′). Whereas the behavior observed with m2 and m1del46 is qualitatively the same as with m1, the limited extent of variation and the relatively high uncertainty of the derived parameters prevented a meaningful quantitative analysis.

However, the approach could be used to obtain an estimate of δ in the case of DIDS and m2 9554. Fig. 6, *B* through *D*, presents the relevant plots. The fit of the K_D versus *V* plot in Fig. 6 *D* according to Eq. 2 (see Materials and Methods) yields $\delta = 0.19 \pm 0.03$, close to the value obtained for m1 17874 (Tombola et al., 2000). Thus, the binding site for DIDS appears to be located approximately in the same region of the channel in VacA m2 as in m1, suggesting a similar structure.

At the single-channel level, m2 9554 (Fig. 7) and m1del46 (Fig. 8) are at least superficially similar to m1 17874 (see Tombola et al., 1999a). All three toxins formed low-conductance channels with a bursting behavior. The gating associated with the fast kinetic mode was extremely rapid, and reliable measurements of the "instantaneous" current conducted could only be obtained using high (4–5 kHz) filter corner frequencies and digitizing rates. The kinetics of the slow mode varied from experiment to experiment, and they were only slightly influenced by voltage (compare amplitude histograms at positive and negative voltage in Figs. 7 and 8).

Channels with different conductances were formed at least by VacA 9554 and by VacA 17874. This is indicated by the variable position of the peaks of point current amplitude histograms produced by different channels under the same conditions (Fig. 7 *J*) and by direct observation of current traces. In several cases the histograms collecting the current conducted by the open, flickering channels required two Gaussians for an adequate fit. In traces recorded at high filter corner frequencies, lower conductance channels on rare occasions exhibited brief openings to relatively high current levels, close to those displayed by other single channels under the same conditions (data not shown). These observations suggest that the channels, once formed, can adopt different conductance states, and that transitions from one substate to the other can be infrequent. A comparison of the conductance of the various forms needs therefore to be statistical. Fig. 9 presents all the available single-channel chord conductance values for the three toxin forms, determined as the mean of the current amplitude histograms obtained from experiments performed under homogeneous conditions. A comparison of the plots indicates that 1) the spread of the conductance values is higher for 17874 than for the other two forms and 2) the average chord conductance of m1 VacA 17874 is higher than that of m1del46, which in turn is higher than that of m2.

DISCUSSION

The comparison of the electrophysiological properties of m1 and m2 VacA forms reveals pronounced similarities,

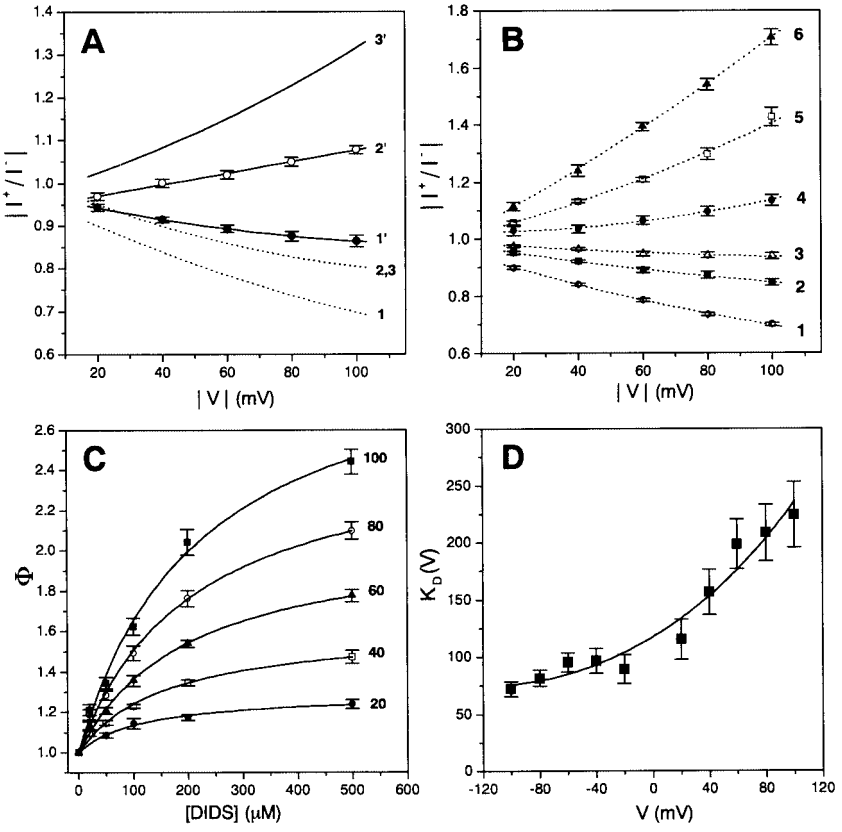

FIGURE 6 Analysis of inhibition. (*A*) Voltage-dependence of inhibition of the three toxin forms by NPPB. Plots of the rectification ratio, $|I^+/I^-|$, versus $|V|$. The three upper curves (numbers with apices) have been determined in the presence of 100 μM NPPB in the *cis* compartment. 1, m2 VacA 9554; 2, m1del46; 3, m1 VacA 17874. The dashed curves 1 and 2 are the best polynomial fits of the data in Fig. 4B. Curves 3 are from Tombola et al. (2000). Curves 2 and 3 without inhibitor coincide. The data with NPPB for m2 9554 (*1′*; ●) and m1del46 (*2′*; ○) are averages from 6 and 10 experiments, respectively. (*B* through *D*) Analysis of the voltage-dependence of the inhibition of m2 VacA 9554 by *cis*-side DIDS. (*B*) Plot of the rectification ratio at various concentrations of DIDS versus $|V|$. The labels 1 to 6 correspond to 0, 20, 50, 100, 200, and 500 μM DIDS, respectively. The data are mean ± SE of three to six determinations ($n = 25$ for curve 1 with no inhibitor). (*C*) Plot of Φ values (see Materials and Methods and Tombola et al., 2000), derived from the data in *B* for the $|V|$ values indicated at the right of the curves, versus [DIDS]. (*D*) Plot of K_D values (± SD) obtained from the fits in *C* versus voltage. All panels, Medium, symmetrical 500 mM KCl.

suggesting that, as expected, the structures of the two pores and the features determining selectivity and voltage-dependence are largely the same. VacA 9554 appears to distinguish less efficiently than the m1 form between cations and anions, and to be slightly more voltage-dependent (Fig. 4), suggesting that the sequence of the m region contributes to determining these properties.

However, a clear-cut difference distinguishes VacA 9554 and m1del46 from m1 VacA 17874 in electrophysiological experiments. As illustrated in Fig. 2, the former two incorporate readily into asolectin membranes but only very reluctantly into planar bilayers formed by DPhPC or PE:PC. m1 VacA 17874 also permeabilizes asolectin membranes more readily, but the difference is much less striking (Fig. 2 *C*). What component(s) of asolectin is responsible for this selectivity remains to be determined. m1 VacA 60190 requires the presence of anionic phospholipids for incorporation (Czajkowsky et al., 1999; Iwamoto et al., 1999) but experiments with mixtures of zwitterionic and negatively charged phospholipids showed that this could not be the explanation for the behavior observed in this study. Recent papers have indicated that interactions with glycosylphosphatidylinositol-anchored (Ricci et al., 2000) and/or (an)other (Yahiro et al., 1997, 1999; Padilla et al., 2000) membrane protein(s), and/or with heparan sulfate (Utt et al., 2001), as well as "aspecific" interactions with the phospholipid bilayer (McClain et al., 2000) may be involved in VacA binding to cells. On the other hand, because the connecting loop is shorter or nonexistent, in all three strongly phospholipid-composition-selective toxins, and because this is the only difference between VacA 17874 and m1del46, a reasonable conclusion is that this structural detail of the protein is responsible for lipid selectivity in our experimental system. This "choosiness" might be associated with a greater structural rigidity, which would hamper the insertion into the membrane of a hydrophobic stretch in the absence of specific interactions. A candidate hydrophobic section is the N-terminal segment. Vinion-Dubiel et al. (1999) have re-

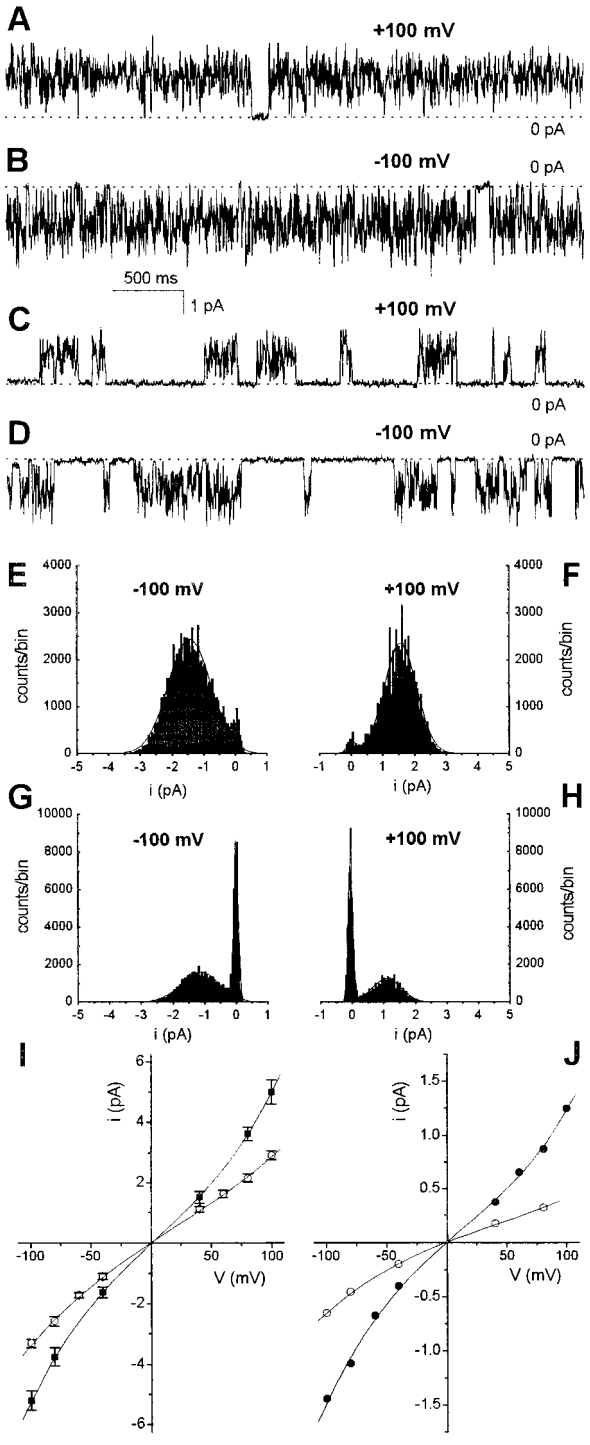

FIGURE 7 m2 VacA 9554 single channels. (*A* and *B*) Channel with high open probability (Po) in the slow kinetic mode. (*C* and *D*) Channel with a relatively low Po in the slow mode. (*E* and *F*) Point current amplitude histograms from the same recordings as in *A* and *B*. (*G* and *H*) Analogous histograms from the records exemplified in *C* and *D*. The histograms are fitted with two Gaussian distributions. The areas under the curves are proportional to the time spent by the channel in the closed mode between bursts (peaks centered at 0 pA) and while bursting. The proportion between these areas remains approximately constant when the voltage is switched from positive to negative, indicating voltage-independence of this gating mode. Membrane, DPhPC; medium, symmetrical 2 M KCl; filter, 100 Hz; sampling, 2 kHz. (*I*) Representative "instantaneous" i/v curves for m2 9554 (○) and m1 17874 (■) channels. The mean ± SE of 20 to 32 (m2) or 17 to 32 (m1) individual measurements at each voltage are plotted. 9554 data were all obtained from one of the highest conductance channels observed (see text). 17874 data are from five distinct channels. The current data were filtered at 4 kHz and digitized at 20 kHz. Other conditions as in *A* through *H*. (*J*) Two representative histogram-based i/v curves for m2 9554. The data plotted are the difference between the peaks of the two Gaussians fitting current amplitude histograms analogous to those in *E* through *H*. Each curve originates from the activity of one channel. Conditions as for *A* through *H*.

ported that deletion of amino acids 6-27 in VacA 60190 results in a protein that oligomerizes, binds to, and is internalized by HeLa cells as well as the parent molecule but has no vacuolating activity and forms channels only with low efficiency. The 6-27 segment seems therefore important for membrane insertion. This hypothesis would also allow a rationalization of the results of de Bernard et al. (1998), who showed that the deletion of a few amino acids at the N terminus made the cytosolically expressed VacA 17874 unable to induce vacuolation. In our scheme, this would be attributed to the ensuing lack of insertion into intracellular membranes (late endosomes).

A further difference is brought to light by the observations at the single channel level. Whereas all three toxins can form channels of various sizes, those produced by m2 9554 have, on average, lower and more narrowly distributed conductances than those of m1 17874 (Fig. 9). As mentioned, the loop connecting the p37 and p58 domains in m2 9554 and m1 60190 is shorter than in m1 17874, and this is thought to lead to preferential hexamer formation. Thus, differences in channel conductance might, a priori, reflect differences in oligomer stoichiometry. Thus, we studied the m1del46 construct, which forms only hexamers (Burroni et al., 1998). The single-channel conductances observed with this protein fall in a range intermediate between those of the 17874 and 9554 toxins (Fig. 9). The average conductance of m1del46 channels is some 23% lower than that of m1 channels. Interestingly, if the percentage of hexamers is taken as 100% for m1del46 and 30% for m1, the channel cross-section is modeled as a regular hexagon or heptagon with a constant side length, and conductance is assumed to be proportional to its area, one calculates an expected decrease of the average conductance by the same amount. These observations suggest that heptamers (as well as hexamers) may form in membranes as well as in solution, producing channels with a somewhat higher mean conductance and more scattered individual values. Alternatively, the higher m1 conductances may arise from hexamers assembled in a different way than m1del46. Other factors evidently intervene to reduce the average conductance of the m2 toxin below that of m1del46. Because the vast majority of the sequence variations between m1 and m2

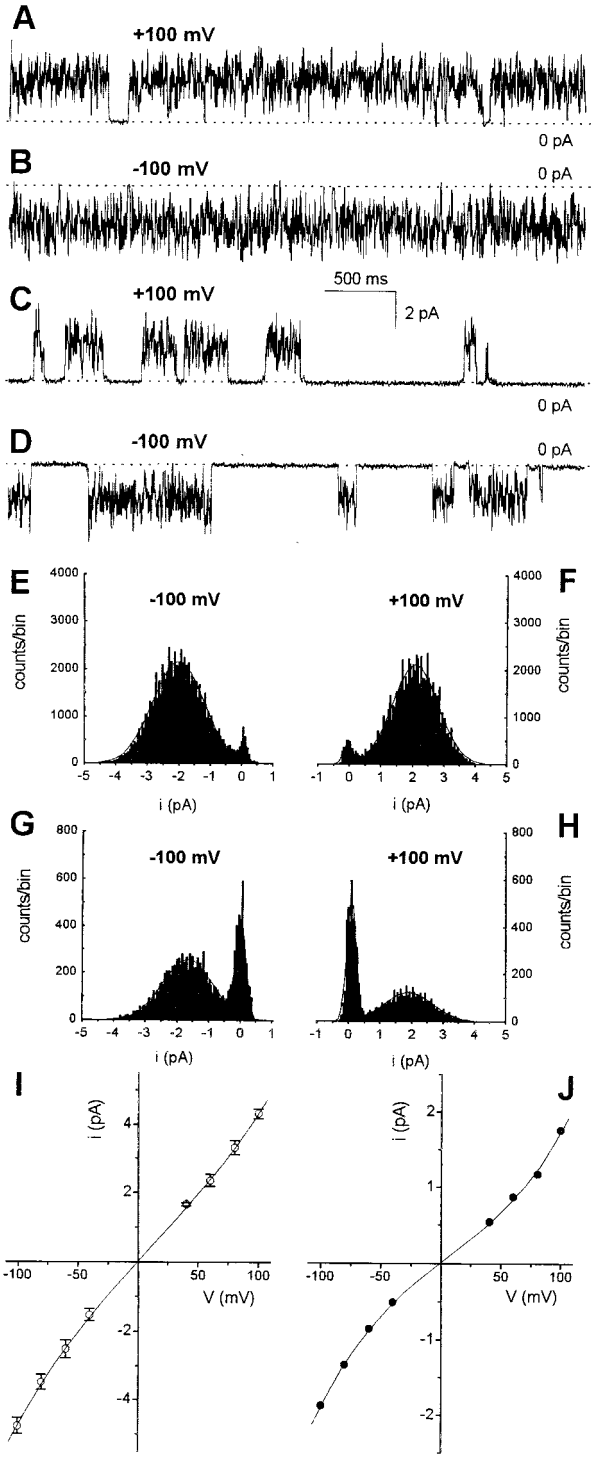

FIGURE 8 VacA m1del46 single channels. Conditions as in Fig. 7. (*A* and *B*) Channel with high Po in the slow kinetic mode. (*C* and *D*) Channel with a relatively low Po in the slow mode. (*E* and *F*) Point current amplitude histograms from the same recordings in *A* and *B*. (*G* and *H*) Histograms from the records exemplified in C and D. (*I*) Representative "instantaneous" i/v curve for m1del46. The data plotted are the averages of 11 to 26 measurements from four experiments (channels). (*J*) Representative histogram-based i/v curve.

forms are concentrated in the m region, it is likely that the characteristics of this region are the major determinant of the conductance of VacA channels.

Our data show that the loop region influences average channel conductance and the propensity of the toxin to enter artificial lipid bilayers. Other recent findings (Pagliaccia et al., 1998; Burroni et al., 1998; Ji et al., 2000) also indicate that it determines structural characteristics of the VacA channel, regulating the stoichiometry of the oligomers. Because m1del46 has essentially the same selectivity and voltage-dependence as the parent molecule (Fig. 4), it seems clear that the length of the loop does not affect these properties, as would be expected of an exposed, domain-connecting strand. The rapid gating of these channels and the existence of various conductance states and of transitions between them imply a certain degree of flexibility of the structure. An influence of the length of the loop is suggested by the narrower distribution of m1del46 conductance values. Furthermore, in 2 of 14 single-channel experiments with this construct we have observed a well-behaved ~20 pS channel completely lacking the fast gating mode (data not shown).

The characterization of inhibition of the three toxin forms by four blockers (Table 1) did not reveal striking differences or clearly identifiable trends. *Cis*-side SITS inhibited m2 VacA 9554 somewhat better than m1 VacA 17874, whereas the opposite was the case for DIDS, NPPB, and IAA-94. The modest quantitative differences presumably reflect details of the interactions between the blockers and their binding sites and/or differences in the rates of entry/exit. Moreover, the similarity of δ^{DIDS} values for m1 and m2 toxins confirms a substantial structural similarity. However, interesting aspects were brought to light by a study of the dependence of inhibition by DIDS on the side of inhibitor addition (the "polarity" or "asymmetry" of inhibition) and of the effect of membrane composition on it. This latter aspect could only be studied using m1 VacA 17874, because the other two proteins did not readily incorporate into nonasolectin membranes.

When DPhPC or PC:PE membranes are used, *trans*-side DIDS inhibits VacA to a still significant extent, although more weakly than when the blocker is added in *cis* (Tombola et al., 2000; Fig. 5 *A*). We have tentatively attributed the lower extent of inhibition from the *trans* side to structural features of the channel (Tombola et al., 2000). When the membrane is made of asolectin, however, *trans*-side DIDS is much less effective (Fig. 5 *A*). This lower effectiveness can be attributed in part to the presence of negatively charged lipids. In fact, the inclusion of 20% negatively charged lipids in PC:PE membranes reduced inhibition, and conversely, addition of poly-lysine to "mask" asolectin charges led to a partial reestablishment of the inhibitory power of *trans*-DIDS in that system (Fig. 5 *B*). Membrane negative charges would be expected to reduce the effective concentration of DIDS, an anion, at the

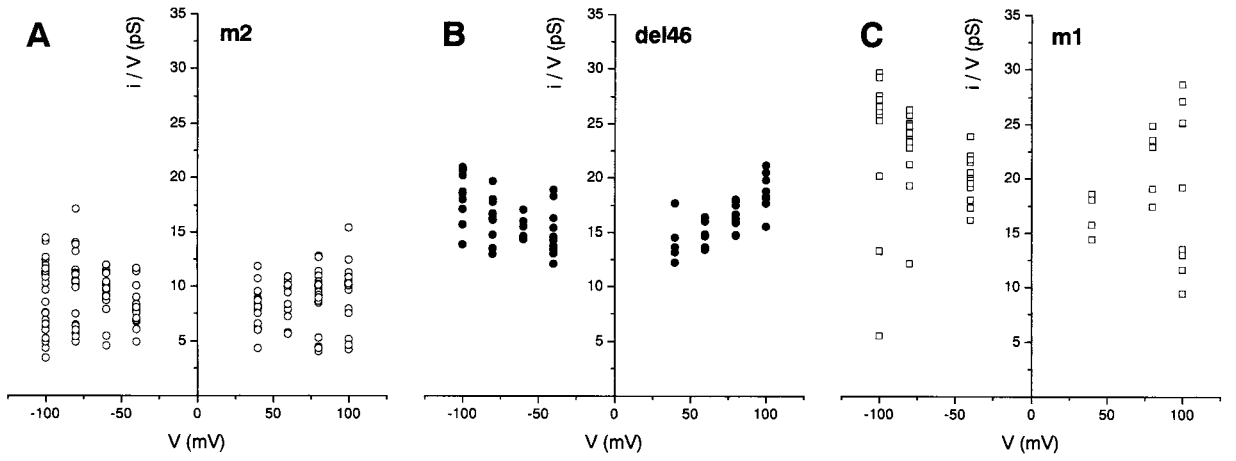

FIGURE 9 Chord conductances of the three VacA forms plotted versus the voltage at which they were determined. (*A*) 139 values for m2 VacA 9554, determined from point current amplitude histograms constructed using 17 separate channels. (*B*) Sixty-seven values for m1del46, from 14 separate channels. (*C*) Sixty values for m1 VacA 17874, originating from 45 different single channels.

membrane-solution interface, because of surface charge effects. On the other hand, in 0.5 M KCl they would be expected to be "shielded" to a large extent. In fact, when DIDS was added on the *cis* side, the change from DPhPC to asolectin had only a minor effect (Fig. 5 *A*). Inhibition by 200 μM *cis*-side DIDS was 1.1-fold higher in DPhPC than in asolectin, whereas the ratio was 6.8 for *trans*-side DIDS (Fig. 5 *A*). When we tested the effect of salt concentration, the K_D for *cis*-side DIDS increased considerably as the ionic strength was lowered. This increase occurred over the whole range of concentrations tested if the membrane was made of asolectin, but in the range 2 to 0.5 M KCl K_D also increased by approximately the same factor when the lipid was DPhPC (Fig. 5 *C*). Ionic interactions between negative charges on the *cis*-side portion of the protein and DIDS, rather than between charges on lipids and DIDS, might account for the K_D changes at higher [salt] in these experiments.

These observations indicate that the low inhibition of asolectin-embedded VacA by *trans*-side DIDS, while linked to the presence of anionic lipids, does not merely reflect ionic interactions between membrane charges and the blocker. We propose, as a working hypothesis, that the origin of this behavior lies in electrostatic interactions between negative charges located on the *trans*-terminal end of the channel and negatively charged membrane lipids. These interactions would favor a conformation with a "more restricted" pore opening, thus limiting access of DIDS to the channel lumen and preventing inhibition. Because the inclusion of PI or PS in an otherwise neutral membrane had only a partial effect, we speculate that the effectiveness of these interactions may depend on details of the structure of the negatively charged membrane components.

Can the differences between m1 VacA 17874 and m2 VacA 9554 observed in electophysiological experiments account for the difference in cytotoxicity? Within the current model of VacA action (Tombola et al., 1999a; Montecucco and Rappuoli, 2001), a lower conductance and selectivity would be expected to make the m2 isoform less powerful a vacuolation agent, mimicking the effect of a partial inhibition of the channels (Szabò et al., 1999). The role of the loop in the cellular model or in vivo is less clear and appears to be minor. Our data suggest a possible role of this portion of the molecule in determining binding to cells at least under some circumstances (Fig. 3) but provide no evidence of an effect on the vacuolation process. The apparent discrepancy between effects on binding and on vacuolation needs to be clarified, but it may be considered to support the notion that only part of the membrane-associated toxin, bound to receptors and thus more readily internalized, is involved in vacuolation (McClain et al., 2000). The further assumption would be required that this "productive" binding depends on the sequence of the m region, but not, or not markedly, on the length of the loop.

In conclusion, we propose that in VacA 17874-specific sets of amino acids in the m region increase the toxin's vacuolating power with respect to m2 isoforms by influencing not only binding but also average conductance, selectivity, and voltage-dependence of the channel.

This work is in partial fulfillment of the requirements for a Doctorate degree in Cellular and Molecular Biology and Pathology by Francesco Tombola. We thank Alessandra Marabese and Laura De Luca for performing part of the experiments, Marina de Bernard for helpful suggestions concerning the ELISA assay, and Ildikò Szabò for critically reading the manuscript. We are also grateful to Prof. Giuseppe Basso (Dept. of Pediatry, University of Padova) for flow cytometry determinations.

This work was supported by CNR, Progetto Finalizzato Biotecnologie (97.01168.PF49), by the National Research Initiative for Advanced Biotechnology (Theme 5), and by Cofin Morst 2000, University of Bari, Bari, Italy.

REFERENCES

Atherton, J. C., P. Cao, R. M. Peek, M. K. Tummuru, M. J. Blaser, and T. L. Cover. 1995. Mosaicism in vacuolating cytotoxin alleles of *Helicobacter pylori*: association of specific VacA types with cytotoxin production and peptic ulceration. *J. Biol. Chem.* 270:17771–17777.

Atherton, J. C., P. M. Sharp, T. L. Cover, G. Gonzalez-Valencia, R. M. Peek, S. A. Thompson, C. J. Hawkey, and M. J. Blaser. 1999. Vacuolating cytotoxin (vacA) alleles of *Helicobacter pylori* comprise two geographically widespread types, m1 and m2, and have evolved through limited recombination. *Curr. Microbiol.* 39:211–218.

Burroni, D., P. Lupetti, C. Pagliaccia, J.-M. Reyrat, R. Dallai, R. Rappuoli, and J. L. Telford. 1998. Deletion of the major proteolytic site of the *Helicobacter pylori* cytotoxin does not influence toxin activity but favours assembly of the toxin into hexameric structures. *Infect. Immunol.* 66:5547–5550.

Cover, T. L. 1996. The vacuolating cytotoxin of *Helicobacter pylori. Mol. Microbiol.* 20:241–246.

Cover, T. L., and M. J. Blaser. 1992. *Helicobacter pylori* and gastroduodenal disease. *Annu. Rev. Med.* 43:135–145.

Cover, T. L., and M. J. Blaser. 1996. *Helicobacter pylori* infection, a paradigm for chronic mucosal inflammation: pathogenesis and implications for eradication and prevention. *Adv. Int. Med.* 41:85–117.

Cover, T. L., P. I. Hanson, and J. E. Heuser. 1997. Acid-induced dissociation of VacA, the *Helicobacter pylori* vacuolating toxin, reveals its pattern of assembly. *J. Cell Biol.* 138:759–769.

Czajkowsky, D. M., H. Iwamoto, T. L. Cover, and Z. Shao. 1999. The vacuolating toxin from *Helicobacter pylori* forms hexameric pores in lipid bilayers at low pH. *Proc. Natl. Acad. Sci. U.S.A.* 96:2001–2006.

de Bernard, M., D. Burroni, E. Papini, R. Rappuoli, J. L. Telford, and C. Montecucco. 1998. Identification of the *Helicobacter pylori* VacA toxin domain active in the cell cytosol. *Infect. Immunol.* 66:6014–6016.

de Bernard, M., E. Papini, V. de Filippis, E. Gottardi, J. L. Telford, R. Manetti, A. Fontana, R. Rappuoli, and C. Montecucco. 1995. Low pH activates the vacuolating toxin of *Helicobacter pylori*, which becomes acid and pepsin resistant. *J. Biol. Chem.* 270:23937–23940.

Hille, B. 1992. Ionic Channels of Excitable Membranes, 2nd ed. Sinauer Associates, Sunderland, MA.

Hotchin, N. A., T. L. Cover, and N. Akhtar. 2000. Cell vacuolation induced by the VacA cytotoxin of *Helicobacter pylori* is regulated by the Rac1 GTPase. *J. Biol. Chem.* 275:14009–14012.

Iwamoto, H., D. M. Czajkowsky, T. L. Cover, G. Szabo, and Z. Shao. 1999. VacA from *Helicobacter pylori*: a hexameric chloride channel. *FEBS Lett.* 450:101–104.

Ji, X., T. Fernandez, D. Burroni, C. Pagliaccia, J. C. Atherton, J.-M. Reyrat, R. Rappuoli, and J. L. Telford. 2000. Cell specificity of *Helicobacter pylori* cytotoxin is determined by a short region in the polymorphic midregion. *Infect. Immunol.* 68:3754–3757.

Lanzavecchia, S., P. L. Bellon, P. Lupetti, R. Dallai, R. Rappuoli, and J. L. Telford. 1998. Three-dimensional reconstruction of metal replicas of the *Helicobacter pylori* vacuolating cytotoxin. *J. Struct. Biol.* 121:9–18.

Leunk, R. D., P. T. Johnson, B. C. David, W. G. Kraft, and D. R. Morgan. 1988. Cytotoxin activity on broth-culture filtrates of *Campylobacter pylori. J. Med. Microbiol.* 26:93–99.

Lupetti, P., J. E. Heuser, R. Manetti, S. Lanzavecchia, P. L. Bellon, R. Dallai, R. Rappuoli, and J. L. Telford. 1996. Oligomeric and subunit structure of the *Helicobacter pylori* vacuolating cytotoxin. *J. Cell Biol.* 133:801–807.

Manetti, R., P. Massari, D. Burroni, M. de Bernard, A. Marchini, R. Olivieri, E. Papini, C. Montecucco, R. Rappuoli, and J. L. Telford. 1995. *Helicobacter pylori* cytotoxin: importance of native conformation for induction of neutralizing antibodies. *Infect. Immunol.* 63:4476–4480.

Marshall, B. J., J. A. Armstrong, D. B. McGechie, and R. J. Glancy. 1985. Attempt to fulfill Koch's postulate for pyloric *Campylobacter. Med. J. Aust.* 142:436–439.

Massari, P., R. Manetti, D. Burroni, S. Nuti, N. Norais, R. Rappuoli, and J. L. Telford. 1998. Binding of *Helicobacter pylori* vacuolating cytotoxin to target cells. *Infect. Immunol.* 66:3981–3984.

McClain, M. S., W. Schraw, V. Ricci, P. Boquet, and T. L. Cover. 2000. Acid activation of *Helicobacter pylori* vacuolating cytotoxin (VacA) results in toxin internalization by eukaryotic cells. *Mol. Microbiol.* 370:1–11.

Molinari, M., C. Galli, M. de Bernard, N. Norais, J. M. Ruysschaert, R. Rappuoli, and C. Montecucco. 1998. The acid activation of *Helicobacter pylori* toxin VacA: structural and membrane binding studies. *Biochim. Biophys. Res. Commun.* 248:334–340.

Montecucco, C., E. Papini, M. de Bernard, J. L. Telford, and R. Rappuoli. 1999b. *Helicobacter pylori* vacuolating cytotoxin and associated pathogenic factors. *In* The Comprehensive Sourcebook of Bacterial Protein Toxins. J. E. Alouf, editor. Academic Press, New York. 264–283.

Montecucco, C., E. Papini, M. de Bernard, and M. Zoratti. 1999a. Molecular and cellular activities of *Helicobacter pylori* pathogenic factors. *FEBS Lett.* 452:16–21.

Montecucco, C., and R. Rappuoli. 2001. Living dangerously: how *Helicobacter pylori* survives in the human stomach. *Nat. Rev. Mol. Cell Biol.* 2:457–466.

Morris, A., and G. Nicholson. 1987. Ingestion of *Campylobacter pyloridis* causes gastritis and raised fasting gastric pH. *Am. J. Gastroenterol.* 82:192–199.

Nguyen, V. Q., R. M. Caprioli, and T. L. Cover. 2001. Carboxy-terminal proteolytic processing of *Helicobacter pylori* vacuolating toxin. *Infect. Immunol.* 69:543–546.

Padilla, I. P., A. Wada, K. Yahiro, M. Kimura, T. Niidome, H. Aoyagi, A. Kumatori, M. Anami, T. Hayashi, J. Fujisawa, H. Saito, J. Moss, and T. Hirayama. 2000. Morphologic differentiation of HL-60 cells is associated with appearence of RPTPβ and induction of *Helicobacter pylori* VacA sensitivity. *J. Biol. Chem.* 275:15200–15206.

Pagliaccia, C., M. de Bernard, P. Lupetti, X. Ji, D. Burroni, T. L. Cover, E. Papini, R. Rappuoli, J. L. Telford, and J.-M. Reyrat. 1998. The m2 form of the *Helicobacter pylori* cytotoxin has cell type-specific vacuolating activity. *Proc. Natl. Acad. Sci. U.S.A.* 95:10212–10217.

Pagliaccia, C., X.-M. Wang, F. Tardy, J. L. Telford, J.-M. Ruysschaert, and V. Cabiaux. 2000. Structure and interaction of *Helicobacter pylori* VacA with a lipid membrane. *Eur. J. Biochem.* 267:104–109.

Papini, E., B. Satin, C. Bucci, M. de Bernard, J. L. Telford, R. Manetti, R. Rappuoli, M. Zerial, and C. Montecucco. 1997. The small GTP binding protein rab 7 is essential for cellular vacuolation induced by *Helicobacter pylori* cytotoxin. *EMBO J.* 16:15–24.

Parsonnet, J. 1998. *Helicobacter pylori*: the size of the problem. *Gut* 43(Suppl. 1):S6–S9.

Pelicic, V., J.-M. Reyrat, L. Sartori, C. Pagliaccia, R. Rappuoli, J. L. Telford, C. Montecucco, and E. Papini. 1999. *Helicobacter pylori* VacA cytotoxin associated to the bacteria increases epithelial permeability independently of its vacuolating activity. *Microbiology.* 142:2043–2050.

Reyrat, J.-M., V. Pelicic, E. Papini, C. Montecucco, R. Rappuoli, and J. L. Telford. 1999. Towards deciphering the *Helicobacter pylori* cytotoxin. *Mol. Microbiol.* 34:197–204.

Ricci, V., A. Galmiche, A. Doye, V. Necchi, E. Solcia, and P. Boquet. 2000. High cell sensitivity to *Helicobacter pylori* VacA toxin depends on a GPI-anchored protein and is not blocked by inhibition of the clathrin-mediated pathway of endocytosis. *Mol. Biol. Cell.* 11: 3897–3909.

Szabò, I., S. Brutsche, F. Tombola, M. Moschioni, B. Satin, J. L. Telford, R. Rappuoli, C. Montecucco, E. Papini, and M. Zoratti. 1999. Formation of anion-selective channels in the cell plasmamembrane by the toxin VacA of *Helicobacter pylori* is required for biological activity. *EMBO J.* 18:5517–5527.

Tombola, F., C. Carlesso, I. Szabò, M. de Bernard, J.-M. Reyrat, J. L. Telford, R. Rappuoli, C. Montecucco, E. Papini, and M. Zoratti. 1999a. *Helicobacter pylori* vacuolating toxin forms anion-selective channels in planar lipid bilayers: possible implications for the mechanism of cellular vacuolation. *Biophys. J.* 76:1401–1409.

Tombola, F., G. Del Giudice, E. Papini, and M. Zoratti. 2000. Blockers of VacA provide insights into the structure of the pore. *Biophys. J.* 79: 863–873.

Tombola, F., F. Oregna, S. Brutsche, I. Szabò, G. Del Giudice, R. Rappuoli, C. Montecucco, E. Papini, and M. Zoratti. 1999b. Inhibition of the

vacuolating and anion channel activities of the VacA toxin of *Helicobacter pylori*. *FEBS Lett.* 460:221–225.

Utt, M., B. Danielsson, and T. Wadstrom. 2001. *Helicobacter pylori* vacuolating cytotoxin binding to a putative cell surface receptor, heparan sulfate, studied by surface plasmon resonance. *FEMS Immunol. Med. Microbiol.* 30:109–113.

Vinion-Dubiel, A., M. S. McClain, D. M. Czajkowsky, H. Iwamoto, D. Ye, P. Cao, W. Schraw, G. Szabo, S. R. Blanke, Z. Shao, and T. L. Cover. 1999. A dominant negative mutant of *Helicobacter pylori* vacuolating toxin (VacA) inhibits VacA-induced cell vacuolation. *J. Biol. Chem.* 274:37736–37742.

Warren, J. R., and B. J. Marshall. 1983. Unidentified curved bacilli on gastric epithelium in active chronic gastritis. *Lancet.* 1:1273–1275.

Woodhull, A. M. 1973. Ionic blockage of sodium channels in nerve. *J. Gen. Physiol.* 61:687–708.

Yahiro, K., T. Niidome, M. Kimura, T. Hatakeyama, H. Aoyagi, H. Kurazono, K. Imagawa, A. Wada, J. Moss, and T. Hirayama. 1999. Activation of *Helicobacter pylori* VacA toxin by alkaline or acid conditions increases its binding to a 250-kDa receptor protein-tyrosine phosphatase β. *J. Biol. Chem.* 274:36693–36699.

Yahiro, K., T. Niidome, M. Kimura, T. Hatakeyama, H. Aoyagi, H. Kurazono, P. I. Padilla, A. Wada, and T. Hirayama. 1997. *Helicobacter pylori* vacuolating cytotoxin binds to the 140-kDa protein in human gastric cancer cell lines, AZ-521 and AGS. *Biochem. Biophys. Res. Commun.* 238:629–632.